electronic reprint

CRYSTALLOGRAPHIC COMMUNICATIONS

ISSN: 2056-9890
journals.iucr.org/e

2-[(4-Chlorophenyl)selanyl]-3,4-dihydro-2*H*-benzo[*h*]chromene-5,6-dione: crystal structure and Hirshfeld analysis

Julio Zukerman-Schpector, Karinne E. Prado, Luccas L. Name, Rodrigo Cella, Mukesh M. Jotani and Edward R. T. Tiekink

Acta Cryst. (2017). E**73**, 918–924

Acta Cryst E CRYSTALLOGRAPHIC COMMUNICATIONS

ISSN 2056-9890

2-[(4-Chlorophenyl)selanyl]-3,4-dihydro-2*H*-benzo[*h*]chromene-5,6-dione: crystal structure and Hirshfeld analysis

Julio Zukerman-Schpector,[a]* Karinne E. Prado,[b] Luccas L. Name,[b] Rodrigo Cella,[b] Mukesh M. Jotani[c] and Edward R. T. Tiekink[d]

[a]Departmento de Química, Universidade Federal de São Carlos, 13565-905 São Carlos, SP, Brazil, [b]Departamento de Engenharia Química, Centro Universitário da FEI, 09850-901, São Bernardo do Campo, São Paulo, Brazil, [c]Department of Physics, Bhavan's Sheth R. A. College of Science, Ahmedabad, Gujarat 380 001, India, and [d]Centre for Crystalline Materials, School of Science and Technology, Sunway University, 47500 Bandar Sunway, Selangor Darul Ehsan, Malaysia. *Correspondence e-mail: julio@power.ufscar.br

Received 12 May 2017
Accepted 22 May 2017

Edited by M. Weil, Vienna University of Technology, Austria

Keywords: crystal structure; selenium; pyran derivative; C—Cl···π interactions; Hirshfeld surface analysis.

CCDC reference: 1551641

Supporting information: this article has supporting information at journals.iucr.org/e

The title organoselenium compound, $C_{19}H_{13}ClO_3Se$ {systematic name: 2-[(4-chlorophenyl)selanyl]-2*H*,3*H*,4*H*,5*H*,6*H*-naphtho[1,2-*b*]pyran-5,6-dione}, has the substituted 2-pyranyl ring in a half-chair conformation with the methylene-C atom bound to the methine-C atom being the flap atom. The dihedral angle between the two aromatic regions of the molecule is 9.96 (9)° and indicates a step-like conformation. An intramolecular Se···O interaction of 2.8122 (13) Å is noted. In the crystal, π–π contacts between naphthyl rings [inter-centroid distance = 3.7213 (12) Å] and between naphthyl and chlorobenzene rings [inter-centroid distance = 3.7715 (13) Å], along with C—Cl···π(chlorobenzene) contacts, lead to supramolecular layers parallel to the *ab* plane, which are connected into a three-dimensional architecture *via* methylene-C—H···O(carbonyl) interactions. The contributions of these and other weak contacts to the Hirshfeld surface is described.

1. Chemical context

The natural product, β-lapachone (see Scheme) can be isolated from the bark of the lapacho tree found in Central and South American countries (see: http://www.beta-lapachone.com/). It exhibits biological activities in the context of cancer (Park *et al.* 2014), being known to induce apoptotic cell-death pathways in a number of cancer cell lines, including breast cancer (Schaffner-Sabba *et al.*, 1984), leukaemia (Chau *et al.*, 1998) and prostate cancer (Li *et al.*, 1995). In an allied application, β-lapachone can be used as a sensitizer in radiotherapy on prostrate (Suzuki *et al.*, 2006) and colon (Kim *et al.*, 2005) cancer cells.

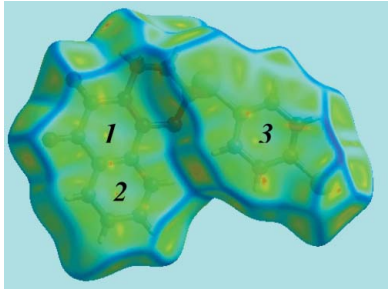

Compounds of the bio-essential element selenium, found in amino acids such as selenocysteine and selenomethionine, are known to hold potential as pharmaceutical agents (Tiekink, 2012), including in the realm of anti-cancer drugs (Seng & Tiekink, 2012). A key aspect of developing metal-based drugs is to incorporate a heavy element into the structure of a biologically active organic molecule and with this in mind, it was thought of interest to attempt to incorporate selenium into the structure of β-lapachone. This was attempted by reacting lawsone, paraformaldehyde and (4-chlorophenyl)-(ethenyl)selane, as detailed in *Synthesis and crystallization*. Two major products were isolated, *i.e.* derivatives of α-lapachone and β-lapachone. The latter, hereafter (I), could be

crystallized and was subjected to an X-ray structure determination along with an analysis of its Hirshfeld surface in order to obtain more information on the molecular packing. The results of this study are reported herein.

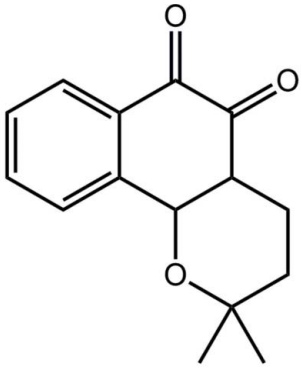

β-Lapachone

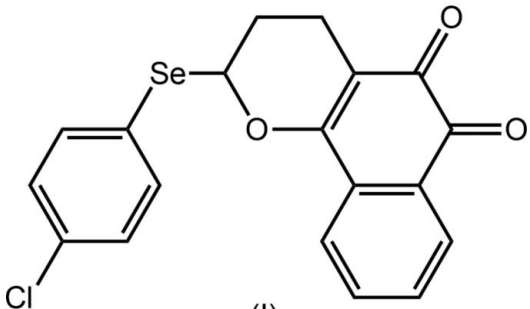

(I)

2. Structural commentary

The substituted 2-pyranyl ring in (I) (Fig. 1) adopts a half-chair conformation with the C13 atom lying 0.620 (3) Å above the plane through the remaining five atoms (r.m.s. deviation = 0.0510 Å). The 12 atoms comprising the naphthalene-1,2-dione ring system are almost coplanar, with an r.m.s. deviation of 0.0152 Å. This plane forms a dihedral angle of 9.96 (9)° with the chlorobenzene ring bound to the selanyl atom, indicating a near parallel disposition and a step-like arrangement between the aromatic substituents about the 2-pyranyl ring. An intramolecular Se···O interaction of 2.8122 (13) Å is noted; this observation is discussed further in the *Database survey*.

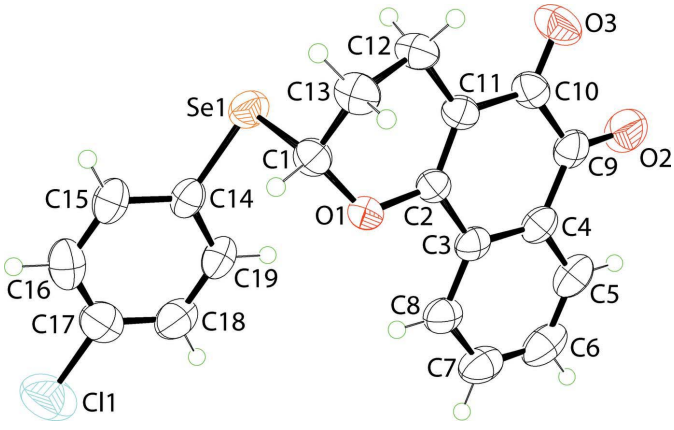

Figure 1
The molecular structure of (I), showing the atom-labelling scheme and displacement ellipsoids at the 50% probability level.

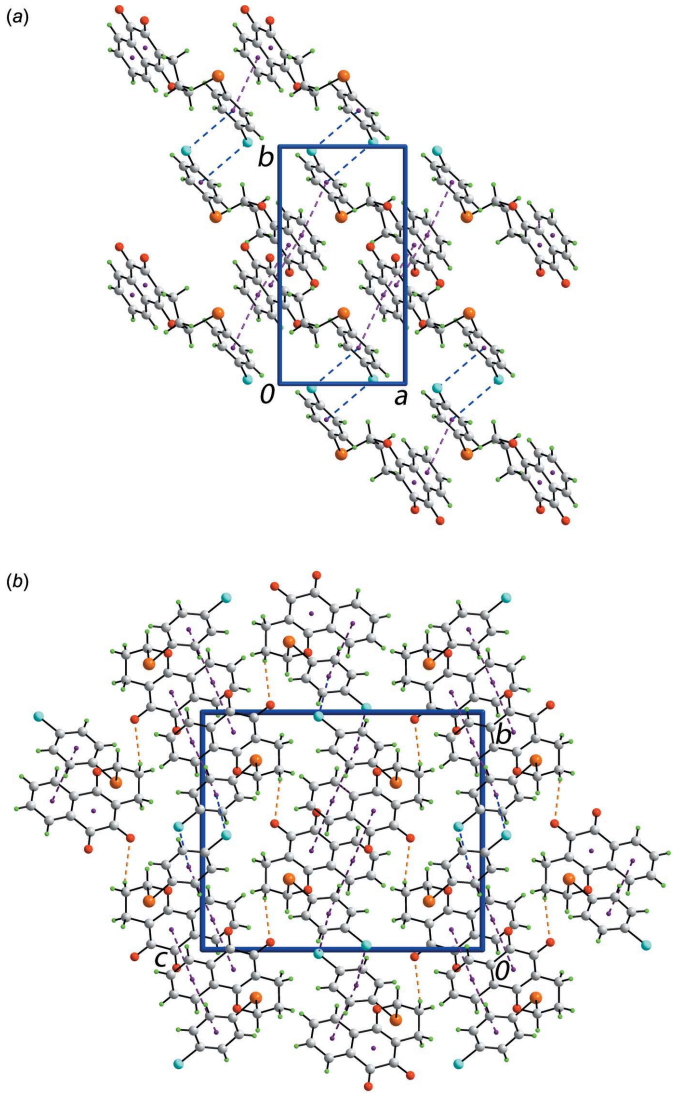

Figure 2
The molecular packing in (I), showing (*a*) a view of the supramolecular layer sustained by π–π and C—Cl···π interactions and (*b*) a view of the unit-cell contents in projection down the *a* axis. The π–π, C—Cl···π and C—H···O interactions are shown as purple, blue and orange dashed lines, respectively.

3. Supramolecular features

In the molecular packing of (I), both rings of the naphthyl residues of centrosymmetrically related molecules form close π–π contacts, *i.e.* *Cg*(C2–C4/C9–C11)···*Cg*(C3–C8)^{i} = 3.7213 (12) Å for an angle of inclination = 0.72 (9)° and symmetry operation (i) $-x, -y, -z$. Two types of interactions connect centrosymmetric aggregates into a supramolecular layer parallel to the *ab* plane (Fig. 2*a*). Thus, π–π interactions

Table 1
Hydrogen-bond geometry (Å, °).

*Cg*1 is the centroid of the C14–C19 ring.

D—H···*A*	*D*—H	H···*A*	*D*···*A*	*D*—H···*A*
C13—H6···O3^{i}	0.97	2.59	3.239 (2)	125
C17—Cl1···*Cg*1^{ii}	1.74 (1)	3.72 (1)	4.000 (2)	86 (1)

Symmetry codes: (i) $-x, y+\frac{1}{2}, -z+\frac{1}{2}$; (ii) $-x+1, -y+1, -z$.

between naphthyl and chlorobenzene rings are formed, [*Cg*(C3–C8)···*Cg*(C14–C19)^{ii} = 3.7715 (13) Å with an angle of inclination = 9.95 (10)° and symmetry operation (ii) $-1+x, y, z$] along with C—Cl···π(chlorobenzene) contacts between centrosymmetrically related rings (Table 1). Connections between layers are of the type methylene-C—H···O(carbonyl) (Table 1) to consolidate the three-dimensional packing (Fig. 2*b*).

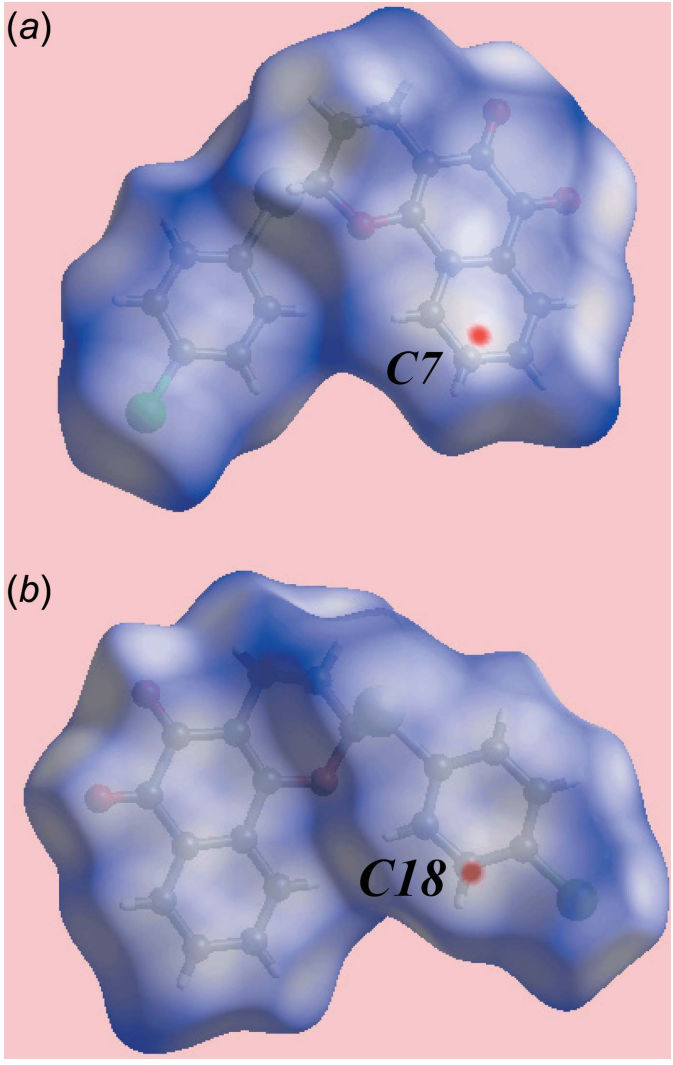

Figure 3
Two views of the Hirshfeld surface for (I) plotted over d_{norm} in the range −0.032 to 1.401 au.

Table 2
Summary of short interatomic contacts (Å) in (I).

Contact	distance	symmetry operation
H5···H11	2.27	$x, \frac{1}{2}-y, \frac{1}{2}+z$
O2···H5	2.70	$-x, -\frac{1}{2}+y, \frac{1}{2}-z$
O3···H9	2.70	$-x, -\frac{1}{2}+y, \frac{1}{2}-z$
C7···C18	3.346 (3)	$-1+x, y, z$

4. Hirshfeld surface analysis

The Hirshfeld surfaces calculated on the structure of (I) also provide insight into the intermolecular interactions; the calculation was performed as in a recent publication (Jotani *et al.*, 2016). The presence of bright-red spots appearing near the naphthyl-C7 and phenyl-C18 atoms on the Hirshfeld surface mapped over d_{norm} in Fig. 3 are due to a short interatomic C···C contact (see Table 2), significant in the crystal of (I). The absence of characteristic red spots near other atoms on the d_{norm}-mapped Hirshfeld surface confirms the absence of conventional hydrogen bonds in the structure except for a weak C—H···O interaction as given in Table 1. The blue and

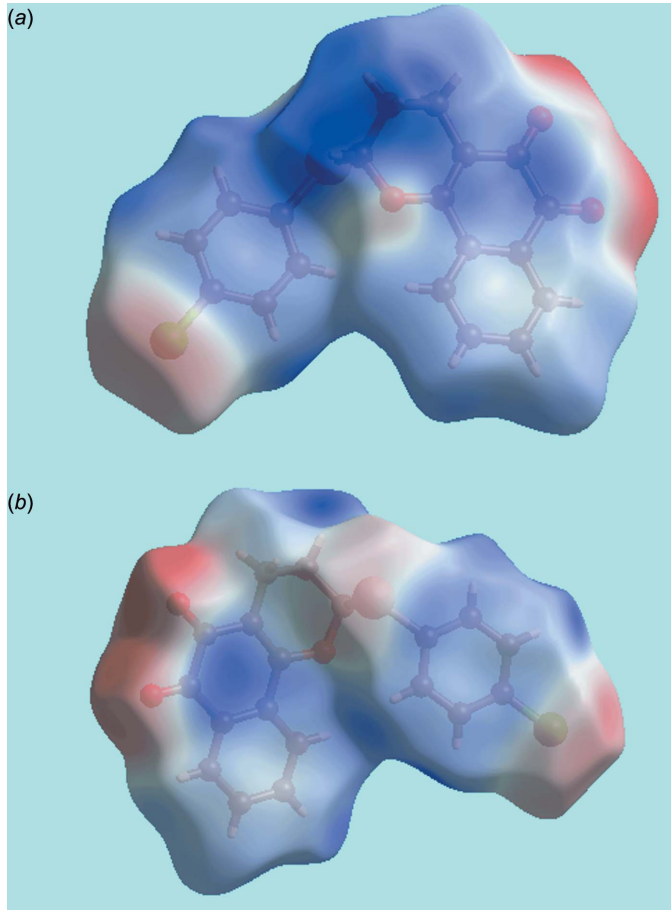

Figure 4
A view of Hirshfeld surface for (I) mapped over the calculated electrostatic potential in the range −0.067 to + 0.039 au. The red and blue regions represent negative and positive electrostatic potentials, respectively.

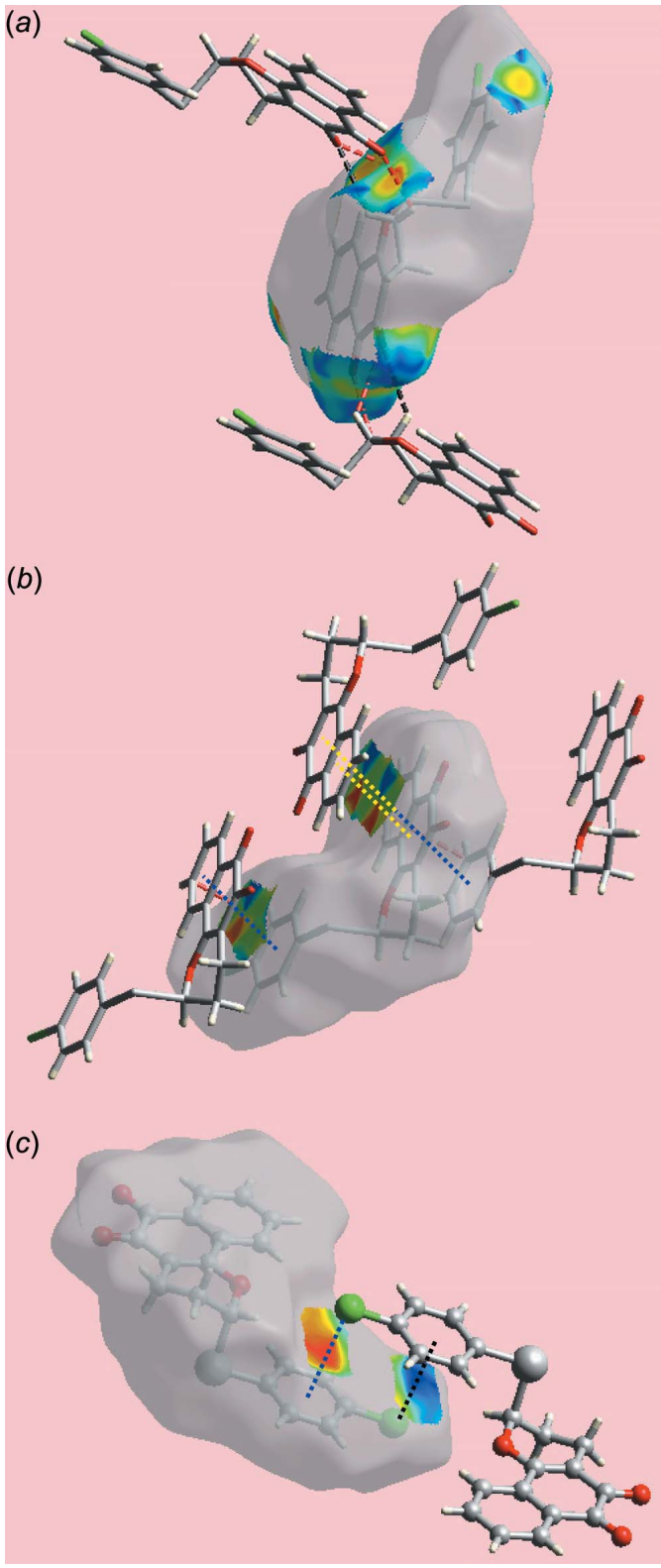

Figure 5
Views of Hirshfeld surfaces mapped over the shape-index about a reference molecule, showing (*a*) C—H···O and short interatomic O···H/H···O contacts by black and red dashed lines, respectively, (*b*) π–π stacking interactions between naphthyl residues and between chlorobenzene and naphthyl rings by blue and yellow dotted lines, respectively and (*c*) C—Cl···π/π···Cl—C stacking contacts between chlorobenzene rings with black and blue dotted lines.

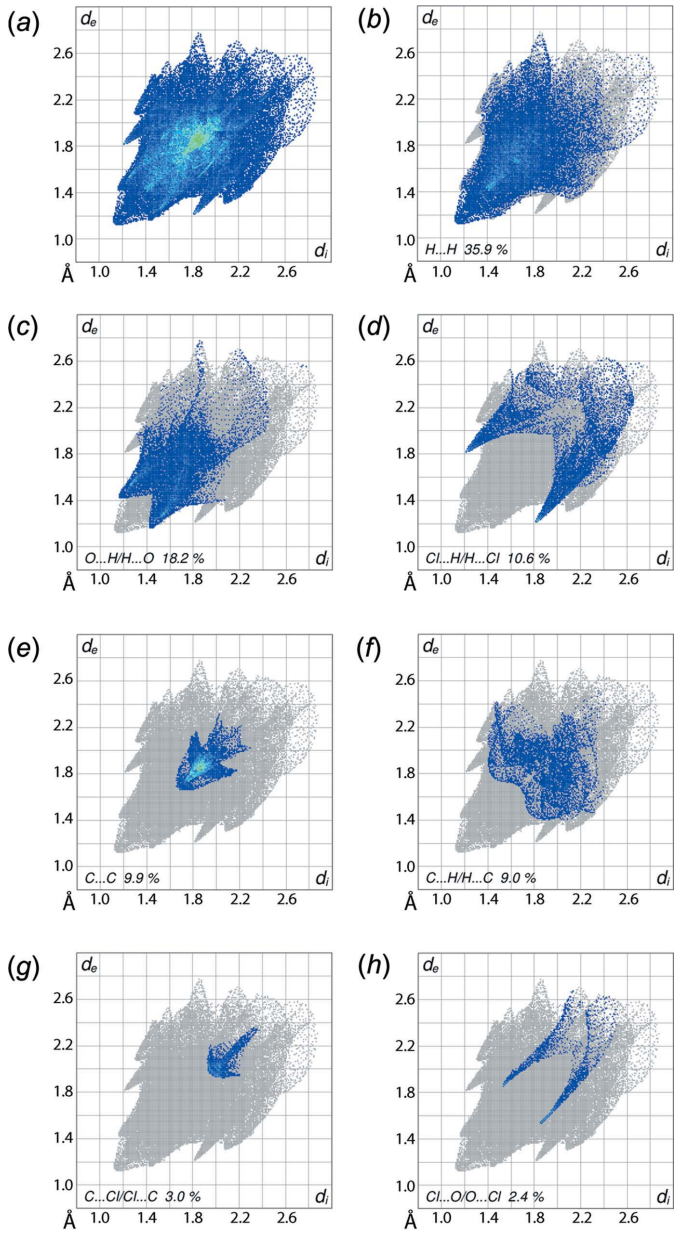

Figure 6
(*a*) The full two-dimensional fingerprint plot for (I) and fingerprint plots delineated into (*b*) H···H, (*c*) O···H/H···O, (*d*) Cl···H/H···Cl, (*e*) C···C, (*f*) C···H/H···C, (*g*) C···Cl/Cl···C and (*h*) Cl···O/O···Cl contacts.

red regions corresponding to positive and negative electrostatic potentials on the Hirshfeld surface mapped over electrostatic potential, in Fig. 4 are the result of polarization of charges localized near the atoms. The immediate environments about a reference molecule within shape-index-mapped Hirshfeld surfaces highlighting intermolecular C—H···O interactions, short interatomic O···H/H···O contacts, π–π stacking interactions and C—Cl···π contacts are illustrated in Fig. 5.

The overall two-dimensional fingerprint plot (Fig. 6*a*) and those delineated into H···H, O···H/H···O, Cl···H/H···Cl, C···C, C···H/H···C, C···Cl/Cl···C and Cl···O/O···Cl

Table 3
Percentage contributions of interatomic contacts to the Hirshfeld surfaces for (I).

Contact	percentage contribution
H···H	35.9
O···H/H···O	18.2
Cl···H/H···Cl	10.6
C···H/H···C	9.0
C···C	9.9
Se···H/H···Se	4.2
Se···C/C···Se	3.0
C···Cl/Cl···C	3.0
C···O/O···C	2.6
Cl···O/O···Cl	2.5
Se···Cl/Cl···Se	0.6
Se···O/O···Se	0.5

contacts (McKinnon *et al.*, 2007) are illustrated in Fig. 6*b*–*h*, respectively; the relative contributions from the various contacts to the Hirshfeld surfaces are summarized in Table 3. The relatively low, *i.e.* 35.9%, contribution from H···H contacts to the Hirshfeld surface of (I) is due to the low content of hydrogen atoms in the molecule and the involvement of some hydrogen atoms in short interatomic O···H/H···O contacts (Tables 1 and 2). The single peak at $d_e + d_i$ ~2.3 Å in Fig. 6*b* is the result of a short interatomic H···H contact (Table 2). The intermolecular C—H···O interaction in the crystal is recognized as the pair of peaks at $d_e + d_i$ ~2.6 Å in the O···H/H···O delineated fingerprint plot (Fig. 6*c*); the points arising from the short interatomic O···H contacts are merged in the plot.

The fingerprint plot delineated into C···C contacts, Fig. 6*e*, characterizes the two π–π stacking interactions, one between inversion-related naphthyl rings, and the other between the chlorobenzene and (C2–C4/C9–C11) rings as the two overlapping triangular regions at around $d_e = d_i$ ~1.8 and 1.9 Å, respectively, having green points in the overlapping portion.

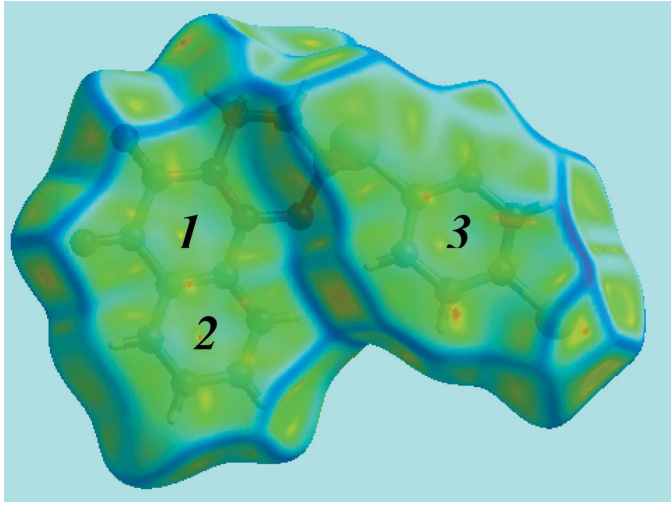

Figure 7
View of the Hirshfeld surface mapped over curvedness highlighting the flat regions corresponding to the C2–C4/C9–C11, C3–C8 and C14–C19 rings, labelled as 1, 2 and 3, respectively, involved in π–π stacking interactions.

The presence of these two π–π stacking interactions is also seen in the flat regions around the participating rings labelled with 1, 2 and 3 in the Hirshfeld surface mapped over curvedness in Fig. 7.

The chlorine atom on the benzene (C14–C19) ring makes a useful contribution to the molecular packing. The small, *i.e.* 3.0%, contribution from C···Cl/Cl···C contacts (Fig. 6*g*) to the Hirshfeld surface is the result of its involvement in a C—Cl···π contact formed between symmetry-related chlorobenzene atoms (Fig. 5*c*). Its presence is also clear from the fingerprint plot delineated into Cl···H/H···Cl (Fig. 6*d*), and Cl···O/O···Cl contacts (Fig. 6*h*). The contribution from C···H/H···C contacts (Fig. 6*f*) and other contacts (Table 3), including the selenium atom, have negligible influence on the packing as the interatomic separations are greater than sum of their respective van der Waals radii.

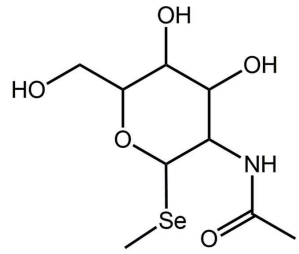

(II)

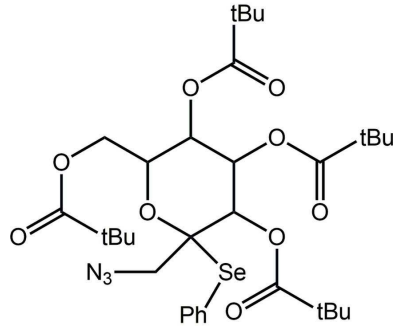

(III)

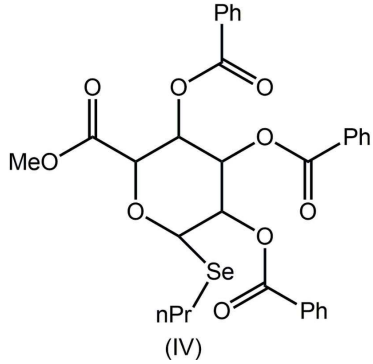

(IV)

5. Database survey

There are three structures in the crystallographic literature (Groom *et al.*, 2016) having a similar 2-(organylselanyl)oxane framework as in (I). The chemical diagrams for these, *i.e.* (II) (Traar *et al.*, 2004), (III) (Woodward *et al.*, 2010) and (IV) (McDonagh *et al.*, 2016) are shown in the Scheme above. Each

Table 4
Summary of Se···O distances (Å) and C—Se—C bond angles (°) in (I)–(IV).

Compound	Se···O	C—Se—C	Ref.
(I)	2.8122 (13)	95.62 (8)	this work
(II)	2.7429 (18)	98.43 (12)	Traar *et al.* (2004)
(III)	2.8760 (12)	98.16 (8)	Woodward *et al.* (2010)
(IV)	2.8606 (19)	97.41 (12)	McDonagh *et al.* (2016)

of the structures features an intramolecular Se···O interaction as in (I). From the data collated in Table 4, there is no correlation between the Se···O distance and the C—Se—C angle, consistent with the weak nature of these interactions.

6. Synthesis and crystallization

Referring to the reaction scheme, in a double-necked flask equipped with a magnetic bar and reflux condenser, under a nitrogen atmosphere, lawsone (1 mmol, 174 mg), paraformaldehyde (8 mmol, 240 mg), the vinyl selenide (1.5 mmol, 326 mg) and the ionic liquid 1-butyl-3-methylimidazolium chloride, [Bmim]Cl (1 mmol, 175 mg) were added over 1,4-dioxane (2 ml). The reaction mixture was heated at 383 K and stirred over 2 h. The reaction mixture was cooled and diluted with dichloromethane (100 ml) and then washed with water (3 × 50 ml). The organic phase was dried over Na_2SO_4, filtered and concentrated under vacuum. The crude product was purified in a silica gel-packed chromatography column, using ethyl acetate and hexane (2:8) as eluent to afford α-lapachone and β-lapachone (I) derivatives in 80% yield. Crystals of (I) were obtained by slow evaporation of a solvent mixture of hexane and ethyl acetate (8:2).

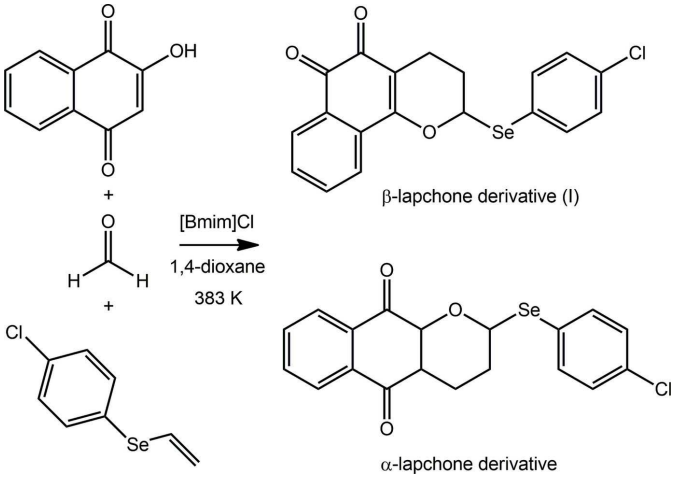

7. Refinement details

Crystal data, data collection and structure refinement details are summarized in Table 5. The carbon-bound H atoms were placed in calculated positions (C—H = 0.93–0.98 Å) and were included in the refinement in the riding-model approximation, with U_{iso}(H) set to 1.2U_{eq}(C).

Table 5
Experimental details.

Crystal data	
Chemical formula	$C_{19}H_{13}ClO_3Se$
M_r	403.70
Crystal system, space group	Monoclinic, $P2_1/c$
Temperature (K)	293
a, b, c (Å)	7.3757 (3), 13.7306 (5), 16.4473 (6)
β (°)	100.002 (1)
V (Å^3)	1640.35 (11)
Z	4
Radiation type	Mo $K\alpha$
μ (mm^{-1})	2.47
Crystal size (mm)	0.40 × 0.33 × 0.27
Data collection	
Diffractometer	Bruker APEXII CCD
Absorption correction	Multi-scan (*SADABS*; Sheldrick, 1996)
T_{min}, T_{max}	0.484, 0.745
No. of measured, independent and observed [$I > 2\sigma(I)$] reflections	38518, 3367, 2984
R_{int}	0.031
(sin $\theta/\lambda)_{max}$ (Å^{-1})	0.626
Refinement	
$R[F^2 > 2\sigma(F^2)]$, $wR(F^2)$, S	0.026, 0.068, 1.03
No. of reflections	3367
No. of parameters	217
H-atom treatment	H-atom parameters constrained
$\Delta\rho_{max}$, $\Delta\rho_{min}$ (e Å^{-3})	0.36, −0.39

Computer programs: *APEX2* and *SAINT* (Bruker, 2009), *SIR2014* (Burla *et al.*, 2015), *SHELXL2014* (Sheldrick, 2015), *ORTEP-3 for Windows* (Farrugia, 2012), *DIAMOND* (Brandenburg, 2006) and *publCIF* (Westrip, 2010).

Acknowledgements

The Brazilian agency National Council for Scientific and Technological Development, CNPq, is gratefully acknowledged for a scholarship to JZ-S (305626/2013–2).

References

Brandenburg, K. (2006). *DIAMOND*. Crystal Impact GbR, Bonn, Germany.
Bruker (2009). *APEX2* and *SAINT*. Bruker AXS Inc., Madison, Wisconsin, USA.
Burla, M. C., Caliandro, R., Carrozzini, B., Cascarano, G. L., Cuocci, C., Giacovazzo, C., Mallamo, M., Mazzone, A. & Polidori, G. (2015). *J. Appl. Cryst.* **48**, 306–309.
Chau, Y. P., Shiah, S. G., Don, M. J. & Kuo, M. L. (1998). *Free Radic. Biol. Med.* **24**, 660–670.
Farrugia, L. J. (2012). *J. Appl. Cryst.* **45**, 849–854.
Groom, C. R., Bruno, I. J., Lightfoot, M. P. & Ward, S. C. (2016). *Acta Cryst.* B**72**, 171–179.
Jotani, M. M., Zukerman-Schpector, J., Madureira, L. S., Poplaukhin, P., Arman, H. D., Miller, T. & Tiekink, E. R. T. (2016). *Z. Kristallogr.* **231**, 415–425.
Kim, E. J., Ji, I. M., Ahn, K. J., Choi, E. K., Park, H. J., Lim, B. U., Song, S. W. & Park, H. J. (2005). *Cancer Res. Treat*, **37**, 183–190.
Li, C. J., Wang, C. & Pardee, A. B. (1995). *Cancer Res.* **55**, 3712–3715.
McDonagh, A. W., Mahon, M. F. & Murphy, P. V. (2016). *Org. Lett.* **18**, 552–555.
McKinnon, J. J., Jayatilaka, D. & Spackman, M. A. (2007). *Chem. Commun.* pp. 3814–3816.
Park, E. J., Min, K.-J., Lee, T.-J., Yoo, Y. H., Kim, Y.-S. & Kwon, T. K. (2014). *Cell Death Dis.* **5**, e1230.

Schaffner-Sabba, K., Schmidt-Ruppin, K. H., Wehrli, W., Schuerch, A. R. & Wasley, J. W. (1984). *J. Med. Chem.* **27**, 990–994.
Seng, H.-L. & Tiekink, E. R. T. (2012). *Appl. Organomet. Chem.* **26**, 655–662.
Sheldrick, G. M. (1996). *SADABS*. University of Göttingen, Germany.
Sheldrick, G. M. (2015). *Acta Cryst.* C**71**, 3–8.
Suzuki, M., Amano, M., Choi, J., Park, H. J., Williams, B. W., Ono, K. & Song, C. W. (2006). *Radiat. Res.* **165**, 525–531.
Tiekink, E. R. T. (2012). *Dalton Trans.* **41**, 6390–6395.
Traar, P., Belaj, F. & Francesconi, K. A. (2004). *Aust. J. Chem.* **57**, 1051–1053.
Westrip, S. P. (2010). *J. Appl. Cryst.* **43**, 920–925.
Woodward, H., Smith, N. & Gallagher, T. (2010). *Synlett*, pp. 869–872.

supporting information

Acta Cryst. (2017). E**73**, 918-924 [https://doi.org/10.1107/S2056989017007605]

2-[(4-Chlorophenyl)selanyl]-3,4-dihydro-2*H*-benzo[*h*]chromene-5,6-dione: crystal structure and Hirshfeld analysis

Julio Zukerman-Schpector, Karinne E. Prado, Luccas L. Name, Rodrigo Cella, Mukesh M. Jotani and Edward R. T. Tiekink

Computing details

Data collection: *APEX2* (Bruker, 2009); cell refinement: *SAINT* (Bruker, 2009); data reduction: *SAINT* (Bruker, 2009); program(s) used to solve structure: *SIR2014* (Burla *et al.*, 2015); program(s) used to refine structure: *SHELXL2014* (Sheldrick, 2015); molecular graphics: *ORTEP-3 for Windows* (Farrugia, 2012) and *DIAMOND* (Brandenburg, 2006); software used to prepare material for publication: *publCIF* (Westrip, 2010).

2-[(4-Chlorophenyl)selanyl]-3,4-dihydro-2*H*-benzo[*h*]chromene-5,6-dione

Crystal data

$C_{19}H_{13}ClO_3Se$
$M_r = 403.70$
Monoclinic, $P2_1/c$
$a = 7.3757$ (3) Å
$b = 13.7306$ (5) Å
$c = 16.4473$ (6) Å
$\beta = 100.002$ (1)°
$V = 1640.35$ (11) Å^3
$Z = 4$
$F(000) = 808$
$D_x = 1.635$ Mg m^{-3}
Mo $K\alpha$ radiation, $\lambda = 0.71073$ Å
Cell parameters from 9049 reflections
$\theta = 2.5$–26.3°
$\mu = 2.47$ mm^{-1}
$T = 293$ K
Irregular, colourless
0.40 × 0.33 × 0.27 mm

Data collection

Bruker APEXII CCD diffractometer
φ and ω scans
Absorption correction: multi-scan (SADABS; Sheldrick, 1996)
$T_{min} = 0.484$, $T_{max} = 0.745$
38518 measured reflections
3367 independent reflections
2984 reflections with $I > 2\sigma(I)$
$R_{int} = 0.031$
$\theta_{max} = 26.4°$, $\theta_{min} = 1.9°$
$h = -9\rightarrow9$
$k = -17\rightarrow17$
$l = -20\rightarrow20$

Refinement

Refinement on F^2
Least-squares matrix: full
$R[F^2 > 2\sigma(F^2)] = 0.026$
$wR(F^2) = 0.068$
$S = 1.03$
3367 reflections
217 parameters
0 restraints
Hydrogen site location: inferred from neighbouring sites
H-atom parameters constrained
$w = 1/[\sigma^2(F_o^2) + (0.0329P)^2 + 0.739P]$ where $P = (F_o^2 + 2F_c^2)/3$
$(\Delta/\sigma)_{max} = 0.001$
$\Delta\rho_{max} = 0.36$ e Å^{-3}
$\Delta\rho_{min} = -0.39$ e Å^{-3}

Special details

Geometry. All esds (except the esd in the dihedral angle between two l.s. planes) are estimated using the full covariance matrix. The cell esds are taken into account individually in the estimation of esds in distances, angles and torsion angles; correlations between esds in cell parameters are only used when they are defined by crystal symmetry. An approximate (isotropic) treatment of cell esds is used for estimating esds involving l.s. planes.

Fractional atomic coordinates and isotropic or equivalent isotropic displacement parameters (Å²)

	x	*y*	*z*	U_{iso}*/U_{eq}
Se1	0.50950 (3)	0.20340 (2)	0.19075 (2)	0.05076 (8)
Cl1	0.74491 (12)	0.48216 (7)	−0.08524 (6)	0.0988 (3)
O1	0.14227 (17)	0.24860 (9)	0.12331 (8)	0.0427 (3)
O2	−0.2776 (2)	−0.07713 (12)	0.09235 (12)	0.0741 (5)
O3	−0.0776 (2)	−0.03054 (10)	0.24246 (10)	0.0628 (4)
C1	0.2739 (3)	0.26958 (13)	0.19618 (12)	0.0429 (4)
H9	0.2967	0.3399	0.1975	0.051*
C2	0.0406 (2)	0.16654 (12)	0.12272 (11)	0.0362 (4)
C3	−0.0687 (2)	0.14639 (13)	0.04065 (11)	0.0389 (4)
C4	−0.1805 (2)	0.06325 (14)	0.02911 (12)	0.0432 (4)
C5	−0.2841 (3)	0.04307 (17)	−0.04809 (13)	0.0563 (5)
H4	−0.3567	−0.0127	−0.0558	0.068*
C6	−0.2792 (3)	0.1060 (2)	−0.11328 (13)	0.0644 (6)
H3	−0.3499	0.0930	−0.1647	0.077*
C7	−0.1698 (3)	0.18762 (19)	−0.10224 (13)	0.0601 (6)
H2	−0.1675	0.2297	−0.1464	0.072*
C8	−0.0625 (3)	0.20824 (16)	−0.02611 (12)	0.0491 (5)
H1	0.0129	0.2630	−0.0197	0.059*
C9	−0.1868 (2)	−0.00345 (14)	0.09908 (13)	0.0468 (4)
C10	−0.0715 (3)	0.02303 (13)	0.18356 (12)	0.0431 (4)
C11	0.0400 (2)	0.10986 (13)	0.19024 (11)	0.0387 (4)
C12	0.1505 (3)	0.13595 (14)	0.27303 (11)	0.0479 (4)
H7	0.2611	0.0965	0.2838	0.057*
H8	0.0787	0.1232	0.3160	0.057*
C13	0.2018 (3)	0.24304 (14)	0.27349 (12)	0.0502 (5)
H6	0.0945	0.2824	0.2774	0.060*
H5	0.2952	0.2568	0.3214	0.060*
C14	0.5784 (2)	0.28761 (13)	0.10819 (12)	0.0433 (4)
C15	0.7139 (3)	0.35717 (15)	0.13040 (13)	0.0508 (5)
H13	0.7709	0.3629	0.1853	0.061*
C16	0.7646 (3)	0.41802 (17)	0.07156 (16)	0.0599 (6)
H12	0.8567	0.4642	0.0862	0.072*
C17	0.6774 (3)	0.40953 (17)	−0.00896 (15)	0.0587 (5)
C18	0.5413 (3)	0.3415 (2)	−0.03203 (14)	0.0617 (6)
H11	0.4824	0.3374	−0.0867	0.074*
C19	0.4930 (3)	0.27935 (17)	0.02638 (13)	0.0527 (5)
H10	0.4034	0.2320	0.0110	0.063*

Atomic displacement parameters (Å²)

	U^{11}	U^{22}	U^{33}	U^{12}	U^{13}	U^{23}
Se1	0.04595 (13)	0.04744 (13)	0.05540 (14)	0.00547 (8)	−0.00095 (9)	0.00375 (9)
Cl1	0.0924 (5)	0.1005 (6)	0.1134 (6)	0.0119 (4)	0.0452 (5)	0.0443 (5)
O1	0.0412 (6)	0.0388 (7)	0.0471 (7)	−0.0011 (5)	0.0046 (5)	0.0103 (6)
O2	0.0652 (10)	0.0486 (9)	0.0975 (13)	−0.0140 (8)	−0.0167 (9)	0.0100 (9)
O3	0.0868 (11)	0.0421 (8)	0.0603 (9)	−0.0118 (7)	0.0148 (8)	0.0101 (7)
C1	0.0477 (10)	0.0305 (8)	0.0495 (10)	0.0001 (7)	0.0056 (8)	−0.0003 (7)
C2	0.0341 (8)	0.0329 (8)	0.0423 (9)	0.0067 (7)	0.0089 (7)	0.0021 (7)
C3	0.0326 (8)	0.0434 (10)	0.0416 (9)	0.0118 (7)	0.0088 (7)	0.0006 (7)
C4	0.0345 (9)	0.0446 (10)	0.0495 (10)	0.0117 (7)	0.0048 (7)	−0.0050 (8)
C5	0.0427 (10)	0.0635 (13)	0.0594 (13)	0.0102 (9)	0.0000 (9)	−0.0145 (11)
C6	0.0501 (12)	0.0963 (19)	0.0437 (11)	0.0186 (13)	−0.0001 (9)	−0.0120 (12)
C7	0.0515 (12)	0.0891 (17)	0.0410 (11)	0.0183 (12)	0.0114 (9)	0.0091 (11)
C8	0.0411 (10)	0.0638 (13)	0.0441 (10)	0.0113 (9)	0.0120 (8)	0.0081 (9)
C9	0.0374 (9)	0.0356 (9)	0.0653 (12)	0.0056 (8)	0.0027 (8)	0.0003 (9)
C10	0.0470 (10)	0.0315 (9)	0.0522 (11)	0.0048 (7)	0.0124 (8)	0.0033 (8)
C11	0.0433 (9)	0.0320 (9)	0.0412 (9)	0.0048 (7)	0.0085 (7)	0.0017 (7)
C12	0.0645 (12)	0.0391 (10)	0.0395 (10)	−0.0009 (9)	0.0076 (9)	0.0026 (8)
C13	0.0664 (13)	0.0386 (10)	0.0458 (10)	−0.0005 (9)	0.0105 (9)	−0.0047 (8)
C14	0.0349 (9)	0.0438 (10)	0.0498 (10)	0.0029 (7)	0.0030 (8)	−0.0071 (8)
C15	0.0432 (10)	0.0541 (12)	0.0536 (11)	−0.0039 (9)	0.0042 (9)	−0.0153 (9)
C16	0.0515 (12)	0.0505 (12)	0.0804 (16)	−0.0078 (10)	0.0189 (11)	−0.0138 (11)
C17	0.0529 (12)	0.0560 (13)	0.0719 (14)	0.0120 (10)	0.0240 (11)	0.0099 (11)
C18	0.0489 (12)	0.0858 (17)	0.0489 (12)	0.0057 (11)	0.0041 (9)	0.0033 (11)
C19	0.0401 (10)	0.0636 (13)	0.0514 (11)	−0.0060 (9)	−0.0006 (9)	−0.0093 (10)

Geometric parameters (Å, º)

Se1—C14	1.918 (2)	C7—H2	0.9300
Se1—C1	1.9769 (19)	C8—H1	0.9300
Cl1—C17	1.742 (2)	C9—C10	1.541 (3)
O1—C2	1.353 (2)	C10—C11	1.442 (3)
O1—C1	1.434 (2)	C11—C12	1.504 (3)
O2—C9	1.208 (2)	C12—C13	1.518 (3)
O3—C10	1.223 (2)	C12—H7	0.9700
C1—C13	1.505 (3)	C12—H8	0.9700
C1—H9	0.9800	C13—H6	0.9700
C2—C11	1.357 (2)	C13—H5	0.9700
C2—C3	1.473 (2)	C14—C15	1.385 (3)
C3—C8	1.395 (3)	C14—C19	1.388 (3)
C3—C4	1.401 (3)	C15—C16	1.379 (3)
C4—C5	1.392 (3)	C15—H13	0.9300
C4—C9	1.478 (3)	C16—C17	1.373 (3)
C5—C6	1.382 (3)	C16—H12	0.9300
C5—H4	0.9300	C17—C18	1.376 (3)
C6—C7	1.375 (4)	C18—C19	1.377 (3)

C6—H3	0.9300	C18—H11	0.9300
C7—C8	1.389 (3)	C19—H10	0.9300
C14—Se1—C1	95.62 (8)	C11—C10—C9	118.81 (16)
C2—O1—C1	117.85 (13)	C2—C11—C10	119.65 (17)
O1—C1—C13	111.73 (16)	C2—C11—C12	121.77 (17)
O1—C1—Se1	110.03 (12)	C10—C11—C12	118.57 (16)
C13—C1—Se1	111.65 (13)	C11—C12—C13	109.32 (15)
O1—C1—H9	107.7	C11—C12—H7	109.8
C13—C1—H9	107.7	C13—C12—H7	109.8
Se1—C1—H9	107.7	C11—C12—H8	109.8
O1—C2—C11	123.53 (16)	C13—C12—H8	109.8
O1—C2—C3	112.17 (14)	H7—C12—H8	108.3
C11—C2—C3	124.29 (16)	C1—C13—C12	110.77 (16)
C8—C3—C4	119.21 (18)	C1—C13—H6	109.5
C8—C3—C2	121.29 (17)	C12—C13—H6	109.5
C4—C3—C2	119.49 (16)	C1—C13—H5	109.5
C5—C4—C3	120.19 (19)	C12—C13—H5	109.5
C5—C4—C9	120.03 (19)	H6—C13—H5	108.1
C3—C4—C9	119.78 (17)	C15—C14—C19	119.8 (2)
C6—C5—C4	119.9 (2)	C15—C14—Se1	119.79 (15)
C6—C5—H4	120.0	C19—C14—Se1	120.39 (15)
C4—C5—H4	120.0	C16—C15—C14	120.3 (2)
C7—C6—C5	120.1 (2)	C16—C15—H13	119.9
C7—C6—H3	120.0	C14—C15—H13	119.9
C5—C6—H3	120.0	C17—C16—C15	119.1 (2)
C6—C7—C8	121.0 (2)	C17—C16—H12	120.4
C6—C7—H2	119.5	C15—C16—H12	120.4
C8—C7—H2	119.5	C16—C17—C18	121.4 (2)
C7—C8—C3	119.6 (2)	C16—C17—Cl1	120.10 (19)
C7—C8—H1	120.2	C18—C17—Cl1	118.46 (19)
C3—C8—H1	120.2	C17—C18—C19	119.6 (2)
O2—C9—C4	122.67 (19)	C17—C18—H11	120.2
O2—C9—C10	119.38 (19)	C19—C18—H11	120.2
C4—C9—C10	117.95 (16)	C18—C19—C14	119.8 (2)
O3—C10—C11	122.40 (18)	C18—C19—H10	120.1
O3—C10—C9	118.79 (17)	C14—C19—H10	120.1
C2—O1—C1—C13	−38.2 (2)	O2—C9—C10—C11	178.44 (18)
C2—O1—C1—Se1	86.38 (16)	C4—C9—C10—C11	−1.4 (2)
C1—O1—C2—C11	8.4 (2)	O1—C2—C11—C10	−179.37 (15)
C1—O1—C2—C3	−171.67 (14)	C3—C2—C11—C10	0.7 (3)
O1—C2—C3—C8	−0.4 (2)	O1—C2—C11—C12	1.8 (3)
C11—C2—C3—C8	179.55 (17)	C3—C2—C11—C12	−178.14 (16)
O1—C2—C3—C4	179.30 (14)	O3—C10—C11—C2	−179.78 (18)
C11—C2—C3—C4	−0.8 (2)	C9—C10—C11—C2	0.4 (3)
C8—C3—C4—C5	−0.1 (3)	O3—C10—C11—C12	−0.9 (3)
C2—C3—C4—C5	−179.83 (16)	C9—C10—C11—C12	179.28 (16)

C8—C3—C4—C9	179.35 (16)	C2—C11—C12—C13	18.3 (3)
C2—C3—C4—C9	−0.3 (2)	C10—C11—C12—C13	−160.59 (17)
C3—C4—C5—C6	−1.0 (3)	O1—C1—C13—C12	57.9 (2)
C9—C4—C5—C6	179.49 (18)	Se1—C1—C13—C12	−65.84 (19)
C4—C5—C6—C7	1.0 (3)	C11—C12—C13—C1	−46.3 (2)
C5—C6—C7—C8	0.2 (3)	C19—C14—C15—C16	−0.2 (3)
C6—C7—C8—C3	−1.4 (3)	Se1—C14—C15—C16	179.92 (16)
C4—C3—C8—C7	1.3 (3)	C14—C15—C16—C17	0.9 (3)
C2—C3—C8—C7	−178.99 (17)	C15—C16—C17—C18	−0.3 (3)
C5—C4—C9—O2	1.0 (3)	C15—C16—C17—Cl1	−177.47 (16)
C3—C4—C9—O2	−178.48 (19)	C16—C17—C18—C19	−1.0 (3)
C5—C4—C9—C10	−179.15 (16)	Cl1—C17—C18—C19	176.26 (17)
C3—C4—C9—C10	1.4 (2)	C17—C18—C19—C14	1.6 (3)
O2—C9—C10—O3	−1.4 (3)	C15—C14—C19—C18	−1.1 (3)
C4—C9—C10—O3	178.77 (17)	Se1—C14—C19—C18	178.81 (16)

Hydrogen-bond geometry (Å, º)

Cg1 is the centroid of the C14–C19 ring.

D—H···*A*	*D*—H	H···*A*	*D*···*A*	*D*—H···*A*
C13—H6···O3^{i}	0.97	2.59	3.239 (2)	125
C17—Cl1···*Cg*1^{ii}	1.74 (1)	3.72 (1)	4.000 (2)	86 (1)

Symmetry codes: (i) −*x*, *y*+1/2, −*z*+1/2; (ii) −*x*+1, −*y*+1, −*z*.